

5 FURTHER CASE HISTORIES

CHAPTER OUTLINE

- ▶ Cavity/old workings detection
- ▶ Detailed pillar detection
- ▶ Near-surface cavity detection
- ▶ Dyke, sill and fault detection
- ▶ In-seam disruptions (lenses, etc.)
- ▶ Coal thickness mapping

This chapter includes a collection of additional case study examples relating to some of the most pertinent coal problems described in this book. Where possible, local coal examples were selected for inclusion, but otherwise the selected examples simply aim to highlight the possible applicability of the method to similar problems in the local coal mining industry.

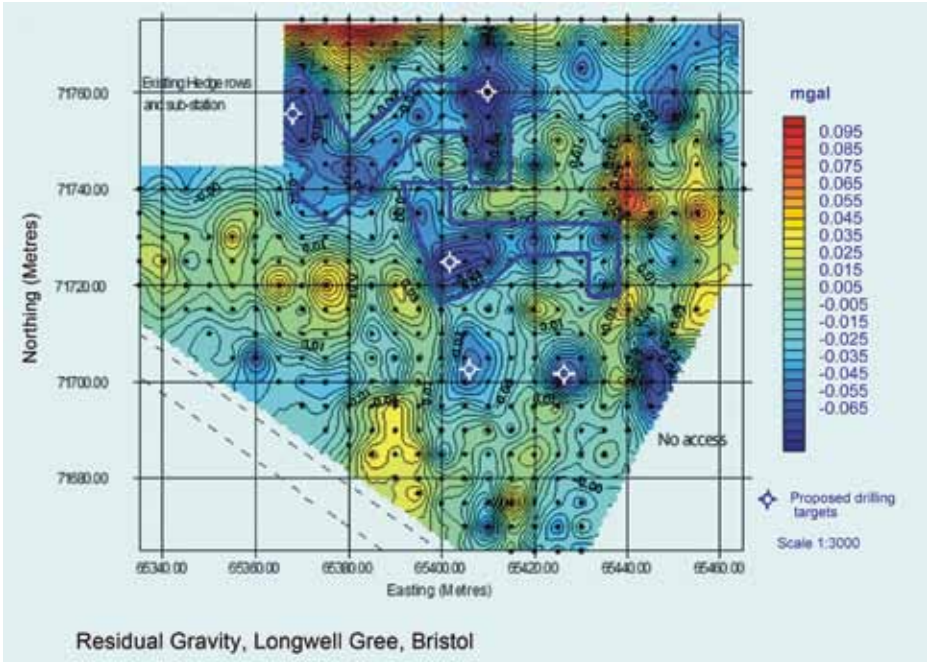
▶ Cavity/old workings detection

Figure 5.1 shows a residual microgravity result acquired over suspected old workings in Bristol, UK⁷². The area outlined in blue represents zones of distinct negative gravity. The subsequent drilling study confirmed the correlation between the low gravity anomalies and old workings occurring at a depth of 12–14 m.

Although there is good correlation between the gravity lows in the output image and the known parts of the old workings, it is clear that the survey was unable to achieve a sufficiently high resolution to confidently and accurately locate the boundaries between mined-out areas and virgin ground.

In 2001/2002 a small-scale microgravity survey was conducted at Kromdraai Colliery near Witbank, aimed at testing whether the method could map the boundary between virgin ground and the old 1 Seam workings, and also whether individual bords and pillars could be mapped. As with the UK example, the old workings lay at a depth of 12–14 m. It can be seen in the survey result shown in Figure 5.2 that the method succeeded in the first goal, but not the second. The resolution of observed anomalies is simply not high enough to enable the delineation of individual bords and pillars. A further drawback of the microgravity method is that data acquisition is a somewhat slow and tedious process.

Figure 5.1 Example of a microgravity survey conducted over suspected old workings in Bristol, UK⁷²



The blue polygon represents the outlines of known parts of the old workings

Figure 5.2 Local microgravity survey example conducted over known bord-and-pillar workings at Kromdraai Colliery, South Africa

Note how the north-eastern extension of the survey grid reveals a clear crossover from low gravity values (blue-green) to high gravity values (red-magenta); this crossover coincides with the edge of workings

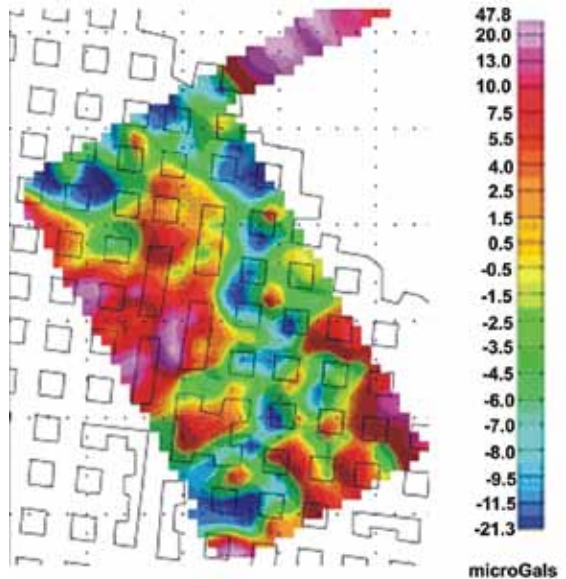
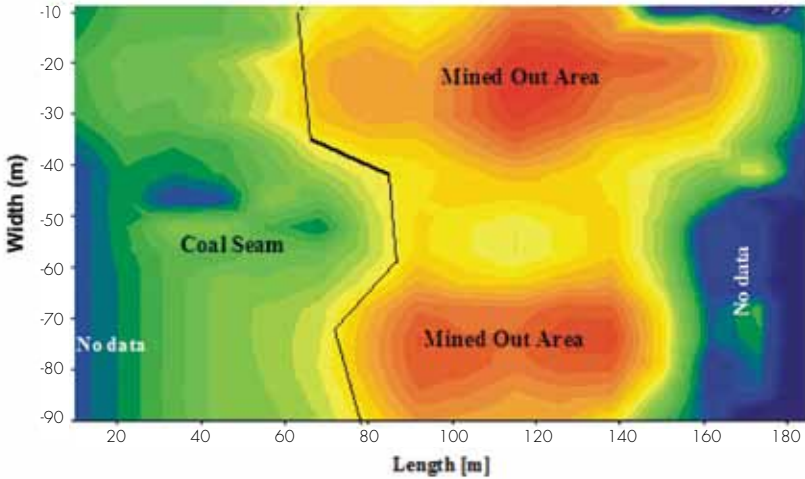
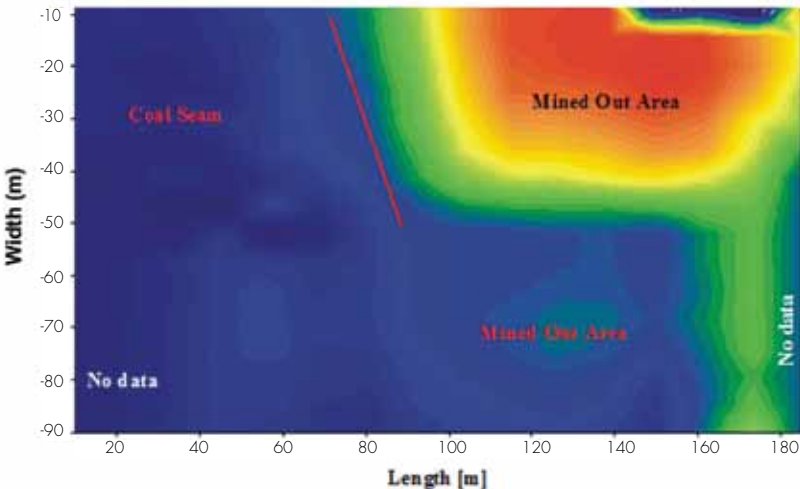


Figure 5.3 shows TDEM results acquired over flooded workings at Arthur Taylor Colliery. This survey formed part of a Coaltech study in 2002. The water-filled workings at a depth of approximately 30 m constituted a good EM target, and the known boundary between flooded workings and virgin ground was located with reasonable accuracy. In this figure, a couple of time slices are shown that correspond approximately with the seam depth. The conductive mine water gives the flooded workings a significantly higher bulk conductivity than the unmined coal seam.

Figure 5.3 TDEM time slices recorded at Arthur Taylor Colliery
Signal Distribution at Time 12.5 μ s



Signal Distribution at Time 30 μ s

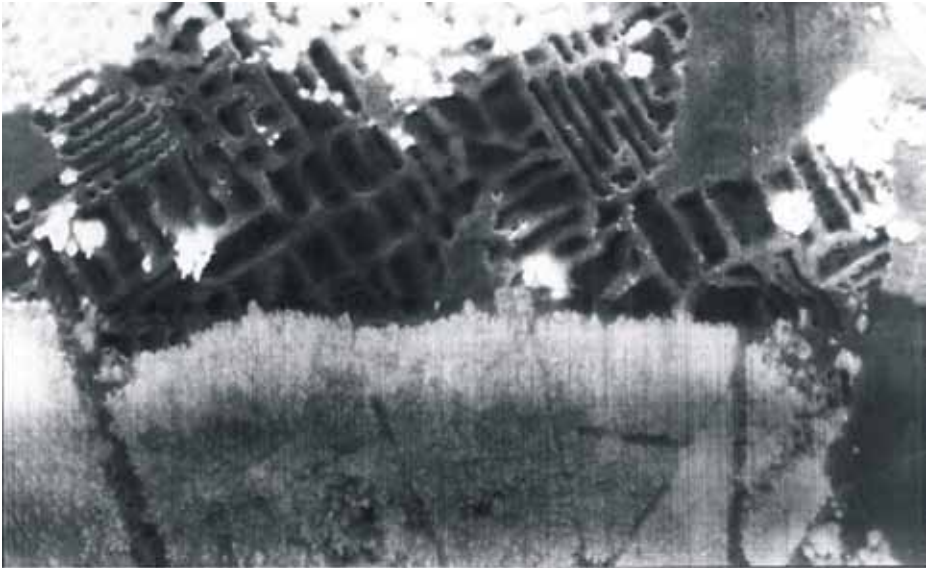


The warm colours (red-orange) represent zones of high conductivity; that is, flooded workings. The colder colours (blue-green) represent the electrically more resistive unmined seam.

► Detailed pillar detection

Figure 5.4 shows a classic example of a successful airborne thermal imagery survey over old workings. The output clearly shows the individual bords and pillars in the top part of the image. However, this example represents a best case scenario where the old workings were located very close to the surface (only a few metres deep). Note also how in places, the presence of vegetation easily masks the thermal response from the workings. For these reasons, it is expected that airborne thermal imagery will only be applicable to the detailed mapping of old workings in very rare circumstances, that generally do not apply to the Witbank and other major coalfields.

Figure 5.4 Example of a successful high-resolution airborne thermal imagery survey over ultra-shallow old workings



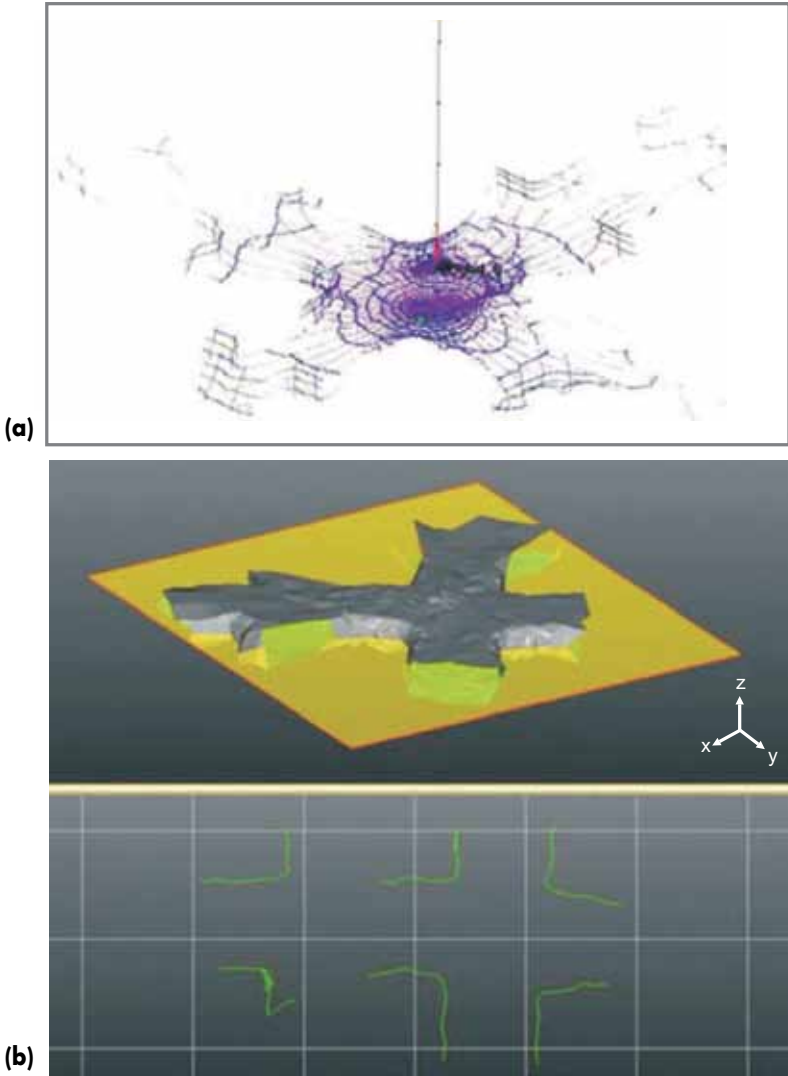
Medium-high temperature zones (grey tones) represent vegetation, while the white blobs (higher temperatures) represent individual tree clusters; the lower temperature areas (black tones) represent collapsed, flooded old bord-and-pillar workings.

Apart from the limited applicability described above, thermal imagery has one other significant disadvantage. The thermal responses and anomalies from targets are generally very small and difficult to distinguish from background responses. For this reason, thermal surveys are usually only effective at certain times of the year and the day, when the thermal contrasts are expected to be greatest.

It was suggested earlier in Chapter 4 that the problem of delineating individual bords and pillars can only be solved effectively by exploiting boreholes that have been drilled into the old workings; for example, by using laser and sonar imaging technologies. The images in Figure 5.5a and b show the results of experimental laser scanning surveys that were recently

done by Optron⁷³ to evaluate this type of approach. Similar experiments for sonar were also being planned at the time of writing. Essentially the outputs from laser and sonar borehole scans are similar; the laser technology, however, is applicable to air-filled cavities, while a sonar scanner is required in flooded workings.

Figure 5.5a and **b** Example of outputs from an experimental three-dimensional borehole laser scanning survey using Optron's CALS system



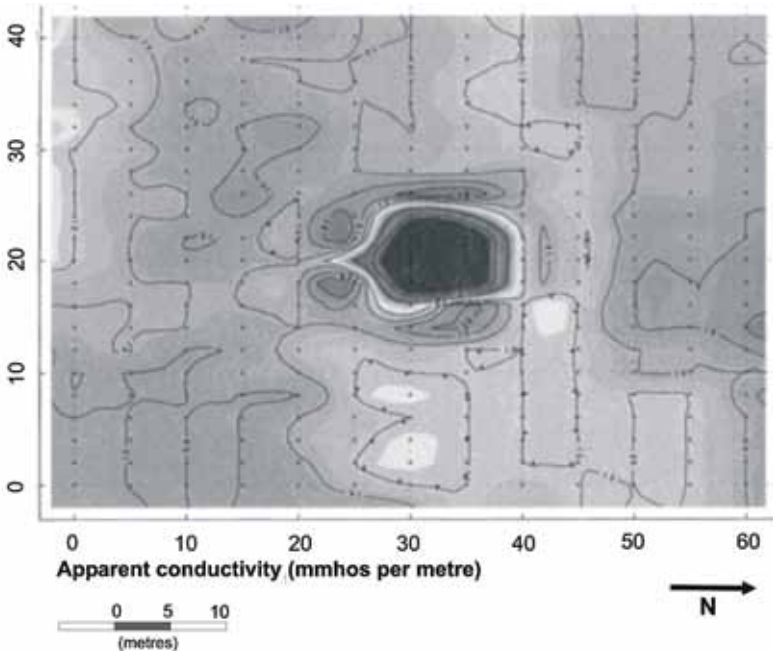
(a) shows a screenshot of the recorded raw data (return reflections);
(b) is a three-dimensional display of bords and pillars derived from the raw data.

An obvious disadvantage of these technologies is that boreholes are required. Furthermore, to reconstruct an accurate representation of the bords and pillars in an area, one needs several strategically placed boreholes. This requires a trial-and-error approach, with the output of the first borehole or two dictating the placement of subsequent boreholes. However, accurate pillar location and geometry information is often needed solely to assess the accuracy and offsets of old mine plans. In this case, periodic single-borehole scans may provide sufficient information to surveyors and mine planners.

► Near-surface cavity detection

It was pointed out in Chapter 4 that a high-resolution EM method may prove the most appropriate solution for mapping isolated near-surface cavities. A similar problem is the search for abandoned mine shafts and tunnels. **Figure 5.6** shows a (ground) EM survey done over an area where a known abandoned mine shaft is buried under spoils⁷⁴. Here, a high-density (2.5 m station spacing) EM-31 grid survey was able to locate clearly the low-conductivity anomaly associated with the subsurface shaft cavity.

Figure 5.6 Example showing the use of a FDM method to detect a buried mine shaft⁷⁴

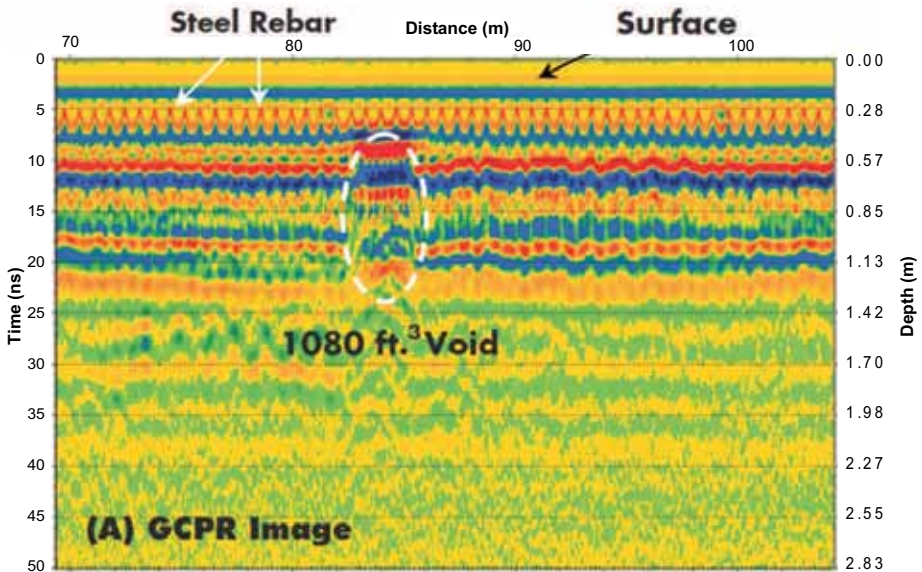


The above example represents a much less challenging task than that of detecting the small, isolated cavities that occur, almost randomly, over previously mined areas. However it illustrates that under favourable conditions and with the appropriate survey parameters, an EM approach may prove very effective. This type of problem will be highly site-specific, and factors such as the target size-to-depth ratio and the properties of the overlying material will influence the applicability of EM methods.

For shallow cavities, the GPR method may prove useful when the properties of the overburden allow for sufficient penetration. GPR is widely used for near-surface cavity detection in fields such as archaeology and civil engineering. **Figure 5.7** illustrates a good example of the latter. It is thought that if the terrain above a previously mined coal area permits the application of three-dimensional GPR surveys, the method may be the most cost-effective way of detecting isolated subsurface cavities. There are unfortunately several obstacles to the successful application of GPR in the Witbank and Highveld areas. The most common problem is the relatively high conductivity of the overburden and of individual layers near the surface. These layers will often impede penetration, and the void-detection efforts.

Another problem is caused by surface conditions (vegetation, topography and unsafe/hazardous conditions, etc.) which make standard surface profiling approaches logistically difficult.

Figure 5.7 Case study example showing how near-surface voids can be detected using GPR⁷⁵

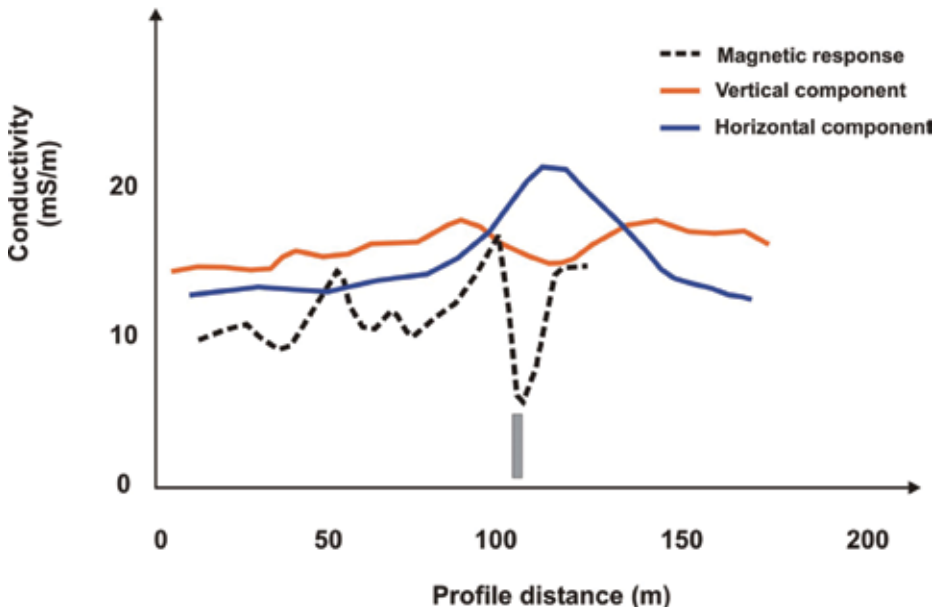


► Dyke, sill and fault detection

Figure 5.8 shows a classic example of the effectiveness of ground magnetics and EM in the detection of dykes. The magnetic response of this vertical dyke with a width of ~ 5 m shows a clear anomaly. The horizontal component of the EM response (shallow depth of investigation), detects the weathered material (clay) at the top of the dyke as a relatively conductive feature, while the vertical component (greater depth of investigation), detects the unweathered deeper part of the dyke as a resistive feature.

Ground EM methods, or a combination of ground EM and magnetics, are good options for detecting intrusions and fault structures on a small scale. These methods may, however, become expensive where larger mine- or regional-scale areas need to be covered. The challenges listed previously for GPR regarding challenging or unsafe surface conditions also apply to the application of ground EM and magnetics.

Figure 5.8 Example of ground FDEM and magnetic results over a known vertical dyke (case study provided by CJS Fourie)



Figures 5.9–5.12 demonstrate the power of airborne geophysics, and in particular airborne EM, in cases where a large area needs to be surveyed and where non-magnetic dykes may be present⁷⁶. Figure 5.9 shows a result derived from an airborne magnetic data set; here the first vertical derivative is presented in an effort to enhance linear features. Several magnetic dykes were mapped, as well as various known man-made features such as railway lines and power lines. The same area was surveyed with a helicopter-based EM system (Dighem), (Figures

5.10–5.12). Most of the magnetic dykes were again detected, but the EM method was also able to detect some dykes that were not evident on the magnetic image. This case study also illustrates how flight lines in two orthogonal directions can help to increase spatial resolution and assist in the detection of linear features that have varying orientations.

Figure 5.9 Airborne magnetic results – first vertical derivative image⁷⁶

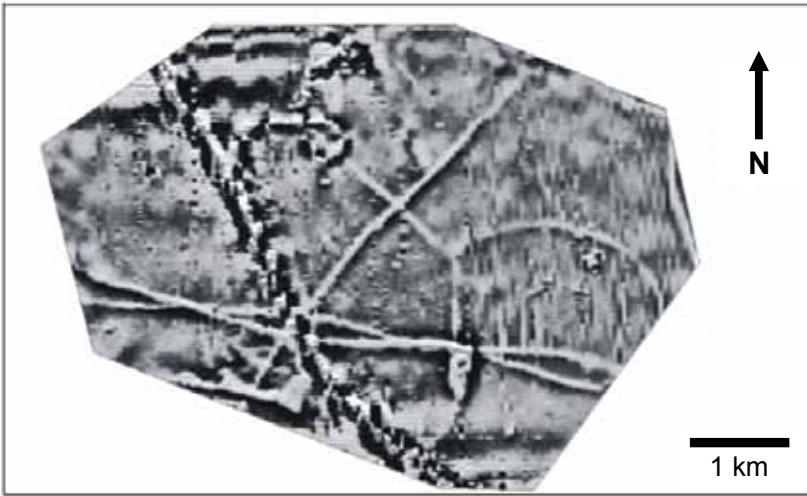


Figure 5.10 Dighem results (7 200 Hz) N-S lines

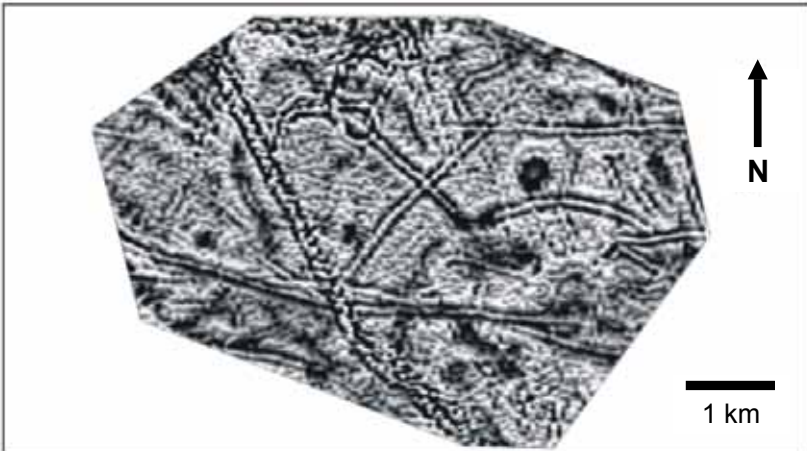


Figure 5.11 Dighem results (7 200 Hz) W-E lines⁷⁶

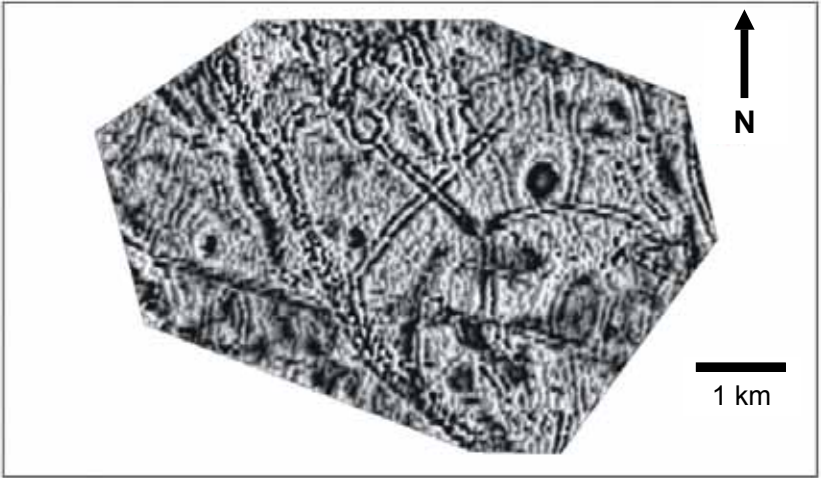


Figure 5.12 Schematic of Dighem survey area showing the major infrastructure and the location of magnetic and non-magnetic dykes⁷⁶



In 2004, the Coaltech Research Organisation commissioned a project (Coaltech Task 1.3.6) to source and merge all available aeromagnetic data sets for the Witbank coalfield⁷⁷. This included over 40 individual data sets from the Coaltech participants and the government (Council for Geoscience). The merged product was subjected to a lineament (dyke) interpretation and results were made available in a GIS-compatible format. **Figures 5.13–5.15** show the key outputs of this exercise.

Figure 5.13 Total field aeromagnetic image for the Witbank coalfield⁷⁷

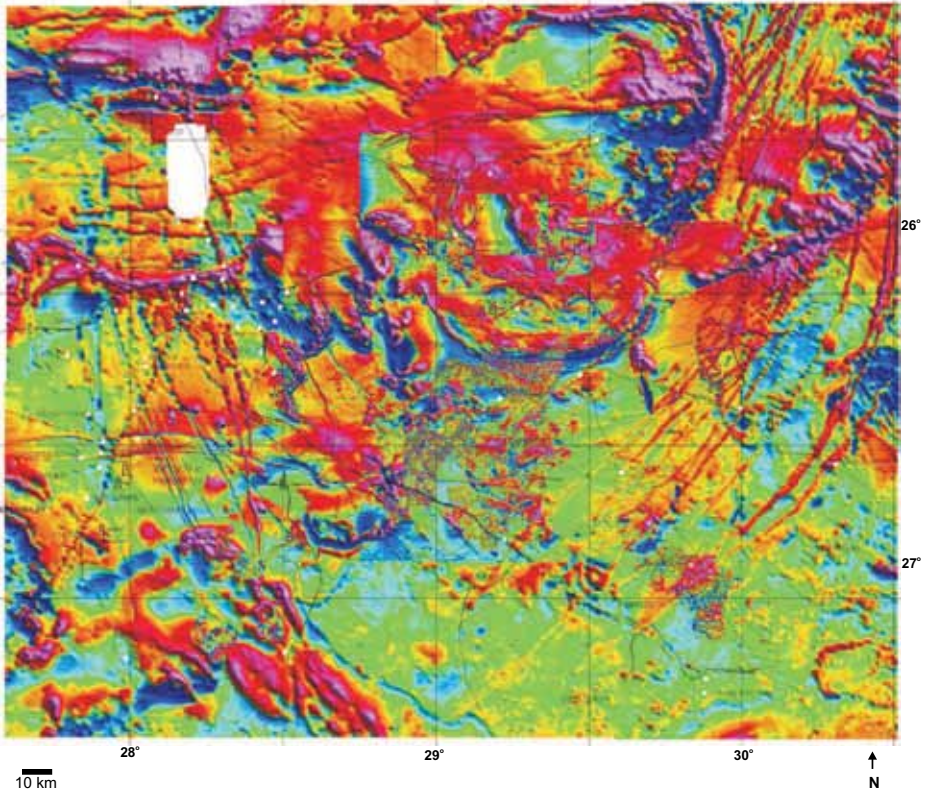


Figure 5.14 First vertical derivative aeromagnetic image of the Witbank coalfield⁷⁷

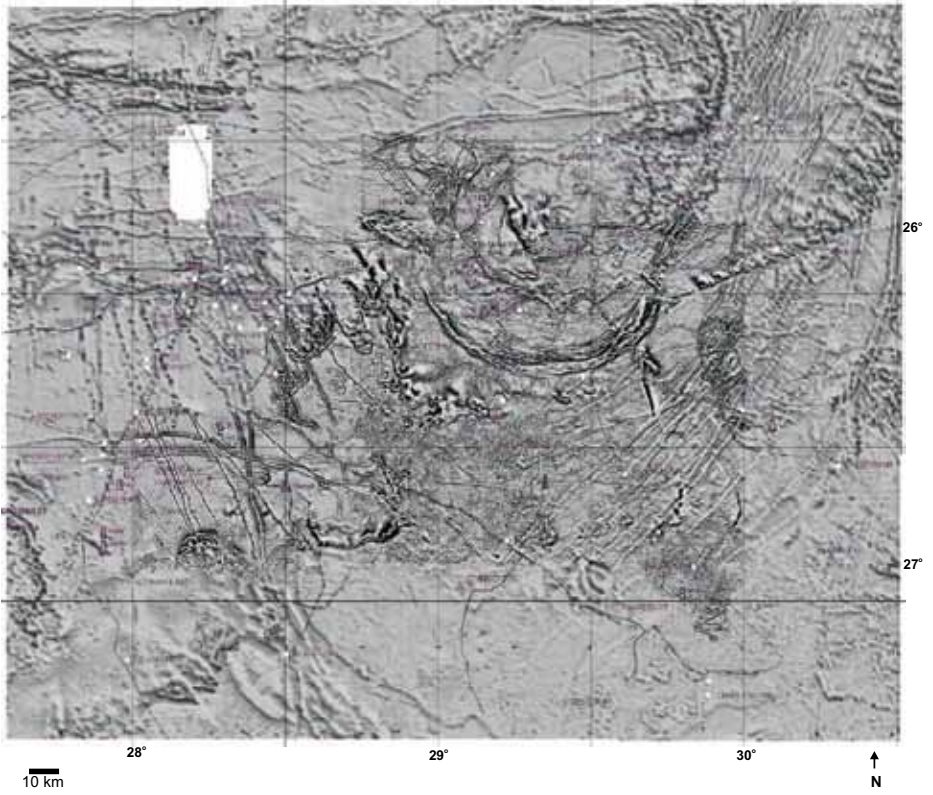
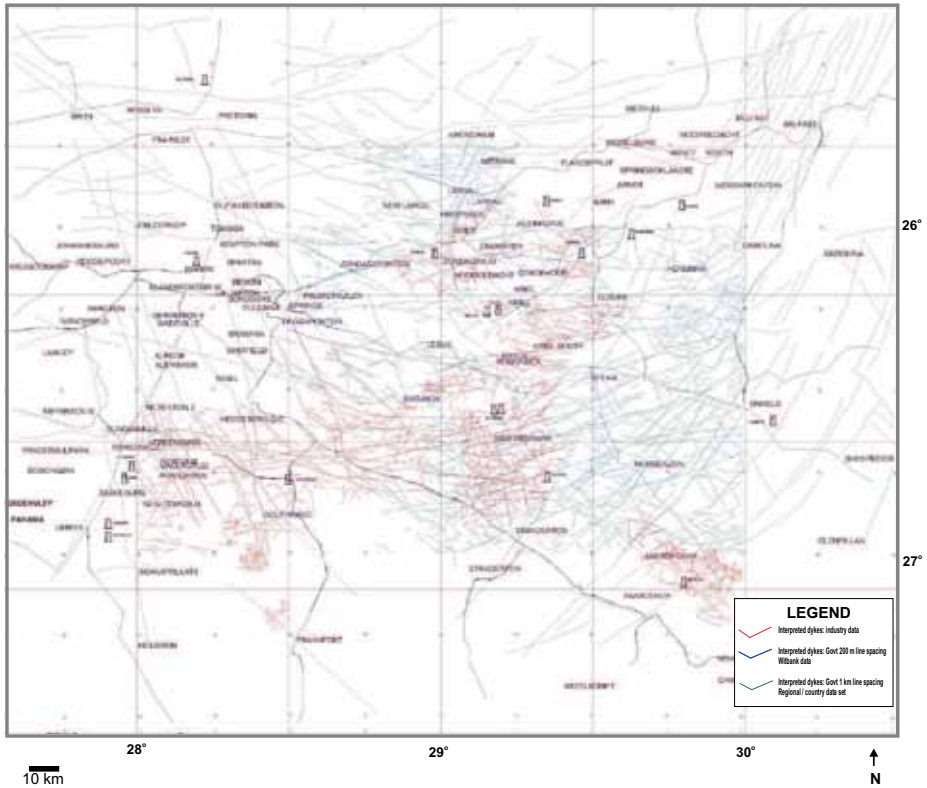
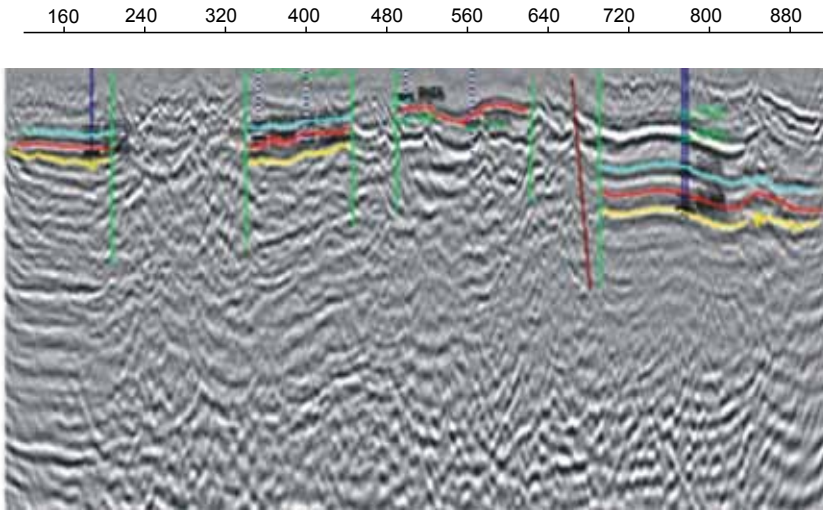


Figure 5.15 Lineament interpretation for the Witbank coalfield for all available aeromagnetic datasets⁷⁷



The seismic reflection method has been used with some success to map coal seam continuity, and especially disruptive features such as faults. Although seismic reflection is expensive and logistically challenging to apply, the method is capable of providing high-resolution images of subsurface layer boundaries down to depths not easily achievable with other conventional geophysical methods. Faults with vertical displacements of as little as 5–10 m, that affect coal seams down to depths of more than 100 m, can in principle be mapped. **Figure 5.16** shows an example from a two-dimensional seismic survey over part of the Witbank coalfield.

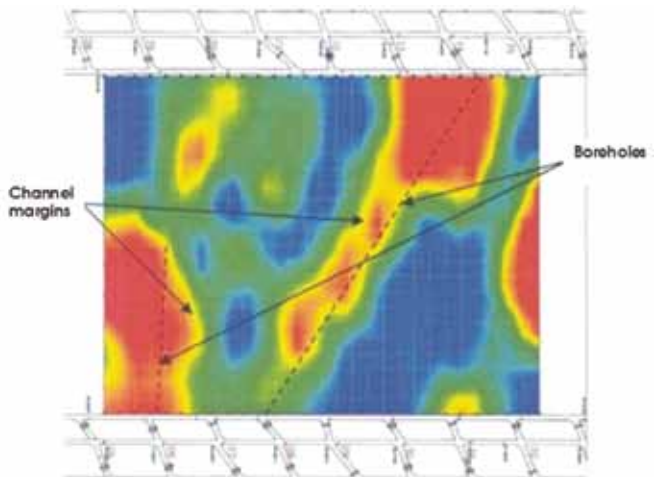
Figure 5.16 Example of a two-dimensional seismic section over a coal mining area
(image provided by Anglo American)



► In-seam disruptions (lenses, etc.)

Non-contact tomographic (imaging) methods that are applied in underground mines – for example, between appropriately located tunnels, boreholes or other developments – can sometimes be used to scan the intervening, unmined seam for disruptive features. For example, the radio imaging method (RIM) has been applied in some parts of the world to map the continuity of coal seams within longwall panels. **Figure 5.17** shows the result of one such successful survey from the USA, aimed at delineating paleochannels in the coal seam ahead of mining. The sandstone channels in this case are associated with an increase in radio wave attenuation – represented by the warmer colours in the image⁷⁸.

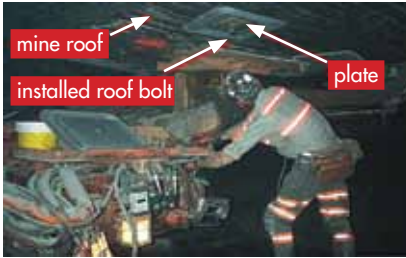
Figure 5.17 Example of a successful in-seam RIM survey from Pittsburgh, USA⁷⁸



► Coal thickness mapping

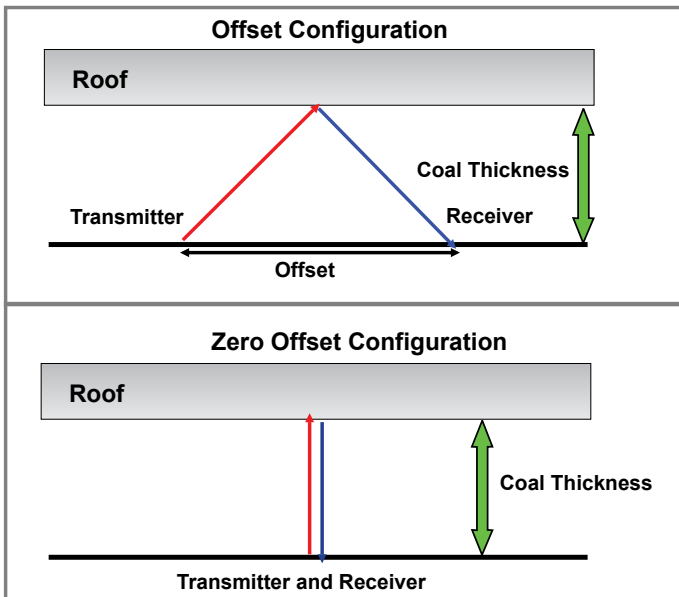
As mentioned in Section 4.3, underground cutters sometimes leave coal behind on the roof, which is then stabilised as a safety precaution by using roof bolts. It is thus of utmost importance that the thickness of the coal is accurately determined so that an adequate roof bolt may be chosen (Figure 5.18).

Figure 5.18 Typical roof bolting scenario



In the past, attempts to solve this problem using radar and electromagnetic techniques have not been successful, and more recently the seismic approach has been investigated. Two possible geometries were considered (Figure 5.19). For the 'offset' option the transmitter (source) and receiver are separated by a certain distance, while the 'zero offset' option implies that the transmitter and receiver are at virtually the same position.

Figure 5.19 Schematic of coal thickness problem and possible survey configurations



A new instrument is currently under development (**Figure 5.20**), which is based on the 'offset' configuration. This development is sponsored by the Coaltech Research Organisation. The technique utilises the two-way travel time of the wave through the coal layer and a knowledge of the seismic velocity of coal to derive the thickness of the coal left behind in the roof. The adopted test instrument is manufactured by Proceq in Sweden. The final underground version will be manufactured from brass contact parts to avoid sparks in the underground environment, and will be made intrinsically safe.

Figure 5.20 Prototype instrument to determine the coal thickness



Tests with the prototype instrument were conducted at Leeuwan Colliery, with the permission of Exxaro. These preliminary tests confirmed that the system is a possible solution to the coal thickness problem and that results are useful if the host rock between the coal seams is either shale or sandstone (**Figure 5.21**). The resolution is better than $0.1\mu\text{sec}$, or 25mm if an average seismic velocity of coal is assumed.

Figure 5.21 Sandstone layers occurring below coal seam at test site



Some laboratory test results are shown in **Figure 5.22**. This test was done to obtain the reflection times and velocities of the relevant geologic materials that will be encountered in underground conditions. At the time of going to press, the field result from Leeuwan was not available in a publishable format.

Figure 5.22 Laboratory test results of Karoo Sandstone

